

Research Article

A Repeatable Optimization for Kinematic Energy System with Its Mobile Manipulator Application

Ying Kong ¹, Ruiyang Zhang,¹ Yunliang Jiang ², and Xiaoyun Xia³

¹Department of Information and Electronic Engineering, Zhejiang University of Science and Technology, China

²School of Information Engineering, Huzhou University, China

³College of Mathematics, Physics and Information Engineering, Jiaying University, China

Correspondence should be addressed to Yunliang Jiang; jyl@zjhu.edu.cn

Received 3 May 2019; Accepted 2 July 2019; Published 31 July 2019

Guest Editor: Chun Wei

Copyright © 2019 Ying Kong et al. This is an open access article distributed under the Creative Commons Attribution License, which permits unrestricted use, distribution, and reproduction in any medium, provided the original work is properly cited.

For repeatable motion of redundant mobile manipulators, the flexible base platform and the redundant manipulator have to be returned to the desired initial position simultaneously after completing the given tasks. To remedy deviations between initial position and desired position of each kinematic joint angle, a special kind of repeatable optimization for kinematic energy minimization based on terminal-time Zhang neural network (TTZNN) with finite-time convergence is proposed for inverse kinematics of mobile manipulators. It takes the advantages that each joint of the manipulator is required to return to the desired initial position not considering the initial orientation of itself for realizing repeatable kinematics control. Unlike the existed training methods, such an optimization of kinematic energy scheme based on TTZNN can not only reduce the convergent position error of each joint to zero in finite time, but also improve the convergent precision. Theoretical analysis and verifications show that the proposed optimal kinematic energy scheme accelerates the convergent rate, which is tended to be applied in practical robot kinematics. Simulation results on the manipulator with three mobile wheels substantiate the timeliness and repetitiveness of the proposed optimization scheme.

1. Introduction

Robot tracking planning of redundant robotic manipulators is to achieve the motion actions to steer the end-effector along with the desired trajectories in the energy optimal system [1–3]. Tracking planning is an important part in engineering robotic applications, such as telecommunication [4], energetic optimization [5], and welding manufacturing [6]. Redundancy of the manipulators is defined as possessing more degrees of freedom (DOF) than the number that the given tasks are required to use. In other words, the end-effector of manipulators will not be able to fulfill a special task if it does not take enough DOF number. The structure of the robot manipulators is tended to be improved with more DOF for the reason of their ability to plan flexible motion trajectory and to optimize different types of kinematic schemes.

Redundant manipulators with fixed base have been investigated by many researchers [7–9]. For expanding the motion

dimension of the manipulators and adding control flexibility of the manipulators, redundant mobile manipulators have been attracted more attention in engineering fields. Due to the unpredicted basements, as compared to the traditional redundant manipulators, the control solutions for trajectory planning give out many difficulties, for example, how to coordinate the relationship between the flexible basement driven by the given tasks and the motion trajectory steered by the integration of the redundant mobile manipulators. How to move to the desired path in time is a considerable problem for inverse kinematics of the mobile manipulators. It is generally known that pseudoinverse solution in joint-velocity formulation is the important method for inverse motion. However, the singularity of each joint angle is not able to be guaranteed when they are moving along the trajectory. Furthermore, each joint angle may not be in their desired initial position after completing the given tasks, which will not yield repetitive motion phenomenon of joint angles. The end-effector of the redundant manipulators may have

difficulties to do the same work when it is demanded for tracking a closed path in the workspace.

To solve these kinematic problems of redundant mobile manipulators, many perfect solving methods have been investigated in many literatures [10–12]. In [13], Tchon proposed a repetitive optimization for kinematic mobile manipulators in engineering fields using endogenous configuration algorithm. However, the joint limits of the manipulators were not considered when the broken phenomenon in mechanism may occur. Miah *et al.* [14] firstly proposed an online optimization algorithm for trajectory moving when the mechanism parameters and measurement error of the nonholonomic differential-drive mobile manipulators were unknown. Tao *et al.* [15] proposed a kind of adaptive neural network model for spacecraft given special tasks in a coordinated control with the consideration of arriving delays and operative uncertainties. In [16], a near-optimal trajectory planning scheme was proposed for receding-wheeled mobile manipulators. Xu [17] proposed a trajectory control method based on neural network for omnidirectional wheeled mobile redundant manipulators with unknown disturbances. In [18], a predictive control scheme with sum-of-squares approach for obstacle avoidance problems in an unknown environment with various polynomial systems was investigated. As the traditional forward kinematics problems concerned, it transformed the joint angles data into Cartesian space with pseudoinverse method for mobile manipulators. However, the solutions for inverse kinematics problems may have many multiple situations and appear deformity of each joint, which is more difficult to be solved directly [19, 20]. Actually, most of the given tasks with the end-effector are in Cartesian while the angular constraint works are in the joint space. How to coordinate the trajectory planning problem in two spaces is worth thinking about especially for inverse motion problem of redundant mobile manipulators.

With the development of neural technologies, a great number of neural networks have been sprung up for the ability of parallel processing, adaptability, memory capacitance, and convenient hardware implementation. Around adaptive neural networks, many research works have been proposed to discuss about. He *et al.* [21] put forward an adaptive neural network model for a health intelligent robot with unknown parameter dynamic system. Chen *et al.* [22] designed an effective adaptive neural network structure for controllers with uncertain information about input parameters and output slide constraints. In literature [23], a prescribed adaptive neural network model characterizing high computation and enough stability was introduced for a disturbed nonlinear system. Recently, with the deep learning of neural networks, a series of network structures are derived around adaptive dynamics. He [24] studied the adaptive fuzzy neural networks for trajectory designing of the mobile manipulators using impedance learning, which effectively integrate the robot arm and the surrounding environment and induce the robotic manipulators to arrive the destination freely. In [25], the adaptive neural network scheme with radial basis function (RBF) was developed to be applied to precision trajectory tracking of distributed movable manipulator device. After the widespread with Gradient recurrent neural network (GNN)

[26], Chen *et al.* [27] proposed a Jacobian-matrix-adaption method based on Zhang neural network for path schematization of the manipulators only considering the input and output parameter information of the robotic models. Furthermore, another kind of recurrent neural network (RNN), which has the powerful energy for multirobot processing, is popularized in redundant mobile manipulators and learning systems [28]. Li *et al.* [29] considered the motion planning for multiple manipulators using distributed neural schemes while all the manipulators can reach the desired position as digital information received. Jin [30] introduced several RNN models from the perspective of control theorem to minimize dynamical error. A type of Zhang neural networks (ZNN) using RNN models is established for solving time-varying calculation problems. Recently, Zhang [31] proposed a varying-parameter Zhang neural network (VP-ZNN), which takes the exponential convergence in robotic engineering fields. In addition, convergence and robustness of VP-ZNN with different activation functions is presented in [32], which is deemed to be applied in repetitive kinematics of manipulators.

There are many solutions for the solving of mechanical kinematics with different types of redundant manipulators. Among these conventional kinematic problems, repetitive movements are often encountered in various engineering areas. Closed path when redundant manipulators have finished the given tasks is the basis of repetitive works especially in the operation process of redundant mobile manipulators. To achieve repetitive motion, a series of Zhang neural networks (ZNN) are proposed, which are formulated as quadratic problems subjected to equation and joint constraints [33–35]. As comparing to the traditional RNN neural methods, ZNN models have the ability of realize the repeatable motion for mobile manipulators as long as time is infinity. As a systematic methodology, zeroing neural dynamic models (ZND) [36–38] have been gradually formulated and situated in many applications, which can avoid the disturbance of internal noise produced by the dynamical systems. In order to shorten the convergent time with ZNN, Li *et al.* [39] firstly introduced a special kind of activation functions to accelerate the convergent speed of ZNN model in finite time, which greatly improved the convergent time. From then on, different ideals about Li's activation function have been studied in literatures and show the finiteness of ZNN combining with this novel nonlinear activated function [40–42]. Motivated by these research results, around the finite-time convergence of ZNN, we investigate a type of terminal-time Zhang neural network (TTZNN), which can reduce the convergent error of dynamic energy system to zero in appointed time. Based on this activation function, a repeatable optimization of kinematic energy system is constructed and systematic theory and finiteness analysis for motion planning of redundant mobile manipulators are provided. Experimental results and comparisons are illustrated the superiority and timeliness of the TTZNN for trajectory tracking of mobile manipulators.

The remainder of this paper is divided into five parts. In Section 2, a kinematic model of redundant mobile manipulator is presented. Section 3 gives out the theoretical

analysis and proof of TTZNN to guarantee the precision and timeliness of the proposed energy system. At the same time, a repeatable motion scheme is established. Stability and convergence of TTZNN are given out in Section 4. In Section 5, numerical simulations are visualized to validate the superiority of TTZNN. Section 6 concludes the paper with future prospects. Finally, the main contributions of this work are listed as follows.

(1) A novel repeatable optimization for kinematic energy system with finite-time convergence based on TTZNN for solving trajectory planning of redundant mobile manipulators is proposed. It is the first time to put forward such a finite-time kinematic criterion, which gives out a new inspiration in the area of robotic manipulator fields.

(2) A terminal-time Zhang neural network (TTZNN) is established for solving repeatable motion planning of mobile manipulators. It is the first time for providing such a neural activation function with finite-time convergence of ZNN as well as in the deep learning of mobile manipulators not considering the initial position of each joint.

(3) The model of the redundant mobile manipulator in this manuscript is the first time to be structured, which is composed of a three-wheel platform and a seven free joints redundant manipulator PA10. It makes a progress in the field for repetitive control of complex mobile manipulators.

(4) Numerical simulation experiments and comparisons with TTZNN optimization scheme of kinematic energy system verified the superiority and timelessness of the proposed trajectory planning optimization. Furthermore, different motion schemes and neural solutions for repeatable motion are compared in the end.

2. Kinematics Structure of Mobile Manipulators

In this section, a mobile manipulation which is composed of a mobile platform with three Swedish wheels and a seven-DOF manipulator PA10 is constructed to demonstrate the real-time of the repetitive motion scheme. The 3D model of the mobile manipulation is visualized in Figure 1. Three Swedish wheels of the mobile platform are all independent. For simplicity, only the end-effector position for given trajectories is considered. In the following paragraphs, the kinematics principle of the mobile platform is analyzed according to the content in literature [43]. Then, the kinematic equation of the PA10 manipulator with seven-DOF joints is given by [44]. Finally, the kinematics modeling of mobile system is obtained combining with the velocity kinematics equation.

2.1. Kinematic Formulation of The Mobile Platform. The geometrical rotation of the mobile base is visualized in Figure 2. Symbols described in Figure 2 are explained as below.

- (1) C : center point of mobile base; the coordinates in base plane are (x_c, y_c, z_c) . Besides, z_c is an invariable constant;
- (2) L : distance between wheels and C ;
- (3) r : radius about each Swedish wheel;

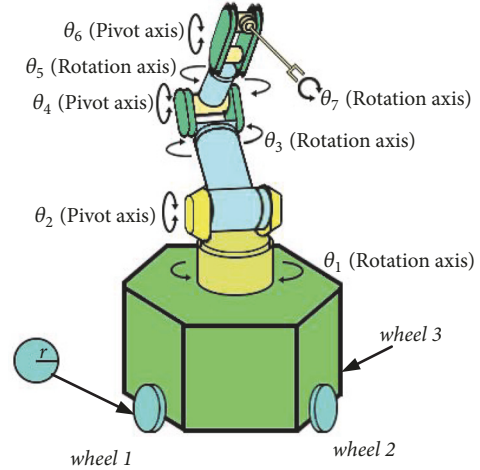


FIGURE 1: 3D integration model of mobile manipulator with three Swedish wheels.

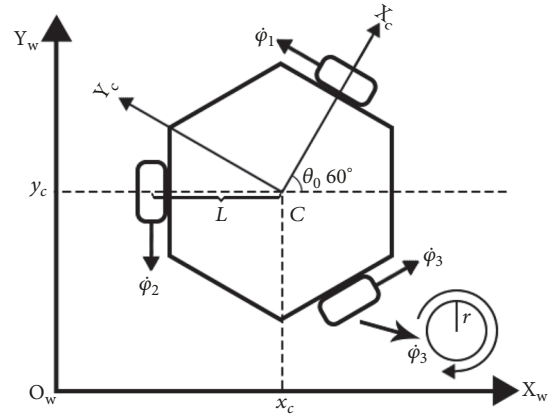


FIGURE 2: Geometrical modeling of the mobile platform.

- (4) θ_0 : heading angle of the kinematic base; angle derivative with time is the velocity $\dot{\theta}_0$;
- (5) $\dot{\phi}_1, \dot{\phi}_2, \dot{\phi}_3$: the rotational velocity of each Swedish wheel.

According to Figure 2, the kinematic formulation of mobile base can be easily got. For the derivative of heading angle with respect to time $\dot{\theta}_0$, we have

$$\dot{\theta}_0 = A\dot{\phi} \quad (1)$$

where $A = [r/(3L), r/(3L), r/(3L)]$ and $\dot{\phi} = [\dot{\phi}_1, \dot{\phi}_2, \dot{\phi}_3]^T$. And for the derivative of point C 's coordinate values with respect to time \dot{x}_c and \dot{y}_c , we have

$$\dot{P}_c = B\dot{\phi} \quad (2)$$

where $\dot{P}_c = [\dot{x}_c, \dot{y}_c]^T$ and B is a matrix related to the heading angle of mobile base θ_0 .

B

$$= \frac{2}{3}r \begin{bmatrix} -\sin(\theta_0) & -\sin\left(\frac{\pi}{3} - \theta_0\right) & \sin\left(\frac{\pi}{3} + \theta_0\right) \\ \cos(\theta_0) & -\cos\left(\frac{\pi}{3} - \theta_0\right) & -\cos\left(\frac{\pi}{3} + \theta_0\right) \end{bmatrix} \quad (3)$$

TABLE 1: D-H parameters of PA10.

Joint(rad)	Axis	a_i (m)	α_i (rad)	d_i (m)	θ_i (rad)
θ_1 (Shoulder1)	Rotating	0	$-\pi/2$	0.317	θ_1
θ_2 (Shoulder2)	Pivoting	0	$\pi/2$	0	θ_2
θ_3 (Shoulder3)	Rotating	0	$-\pi/2$	0.45	θ_3
θ_4 (Elbow1)	Pivoting	0	$\pi/2$	0	θ_4
θ_5 (Elbow2)	Rotating	0	$-\pi/2$	0.48	θ_5
θ_6 (Wrist1)	Pivoting	0	$\pi/2$	0	θ_6
θ_7 (Wrist2)	Rotating	0	0	0.07	θ_7

Combining (1) and (2), the following equations can be obtained:

$$\begin{bmatrix} \dot{\theta}_0 \\ \dot{P}_C \end{bmatrix} = \begin{bmatrix} A \\ B \end{bmatrix} \times \dot{\phi} \quad (4)$$

This article takes $r = 0.1$ m and $L = 0.3$ m.

2.2. Kinematics of PA10 Redundant Manipulator. The PA10 manipulator is a redundant robotic arm with seven-DOF joints. For any stationary manipulators, the end-effector matrix vector $r(t)$ is the kinematic path produced by the joint matrix vector $\theta(t)$. The forward equation of the kinematic manipulators is defined as

$$r(t) = f(\theta(t)) \quad (5)$$

In this manuscript, the end-effector vector of PA10 manipulator is written as $r_w(t) = [x_w, y_w, z_w]^T$ and the joint vector of PA10 manipulator is written as $\theta(t) = [\theta_1(t), \theta_2(t), \dots, \theta_7(t)]^T$. The mechanical information about PA10 manipulator can be found in literature [44]. Due to the space limitation, details of each joint for PA10 manipulator are omitted here. The D-H parameters of the PA10 manipulator are listed in Table 1.

2.3. Integration Modeling of The Mobile Manipulator. After understanding the structure of the mobile base and the seven-joint manipulator, the model of the proposed mobile manipulator with three Swedish wheels is formulated by the kinematic integration of PA10 manipulator and the movable platform. In fact, the main difference between mobile manipulators and stationary manipulators is just the movable base. The movable platform may bring uncertainty prospect. Connecting the bottom coordinate system with global coordinate system by using the transformation matrix, an entirely new kinematical control equation based on global coordinate system can be described as follows

$$r_w = \begin{bmatrix} R(\theta_0) & P_C \\ & 0 \end{bmatrix} \begin{bmatrix} f(\theta) \\ 1 \end{bmatrix} = \begin{bmatrix} P_C \\ 0 \end{bmatrix} + R(\theta_0) f(\theta) \quad (6)$$

where $R(\theta_0)$ is the rotation matrix between PA10 manipulator and the mobile platform.

$$R(\theta_0) = \begin{bmatrix} \cos \theta_0 & -\sin \theta_0 & 0 \\ \sin \theta_0 & \cos \theta_0 & 0 \\ 0 & 0 & 1 \end{bmatrix} \quad (7)$$

By differentiating (6) with respect to time t , we have

$$\dot{r}_w = J(\theta_0, \theta) \begin{bmatrix} \dot{\theta}_0 \\ \dot{\theta} \end{bmatrix} + \begin{bmatrix} \dot{P}_C \\ 0 \end{bmatrix} \quad (8)$$

Jacobian matrix $J(\theta_0, \theta)$ is defined as $J(\theta_0, \theta) = \partial g(\theta_0, \theta) / \partial \omega$ with $\omega = [\theta_0; \theta]$. To simplify (8), substituting (4) into (8), (8) can be rewritten as

$$\dot{r}_w = J(\theta_0, \theta) \begin{bmatrix} A\dot{\phi} \\ \dot{\theta} \end{bmatrix} + \begin{bmatrix} B\dot{\phi} \\ 0 \end{bmatrix} \quad (9)$$

Set a vector $\Theta = [\varphi^T, \theta^T]^T$, and $\dot{\Theta} = [\dot{\varphi}^T, \dot{\theta}^T]^T$ is the time derivative of Θ . Equation (9) can be rewritten as follows:

$$\dot{r}_w = \left(J(\theta_0, \theta) \begin{bmatrix} A & 0 \\ 0 & I \end{bmatrix} + \begin{bmatrix} B & 0 \\ 0 & 0 \end{bmatrix} \right) \begin{bmatrix} \dot{\phi} \\ \dot{\theta} \end{bmatrix} = K\dot{\Theta} \quad (10)$$

where I represents the identity matrix and parameter K is a matrix and is defined as

$$K = J(\theta_0, \theta) \begin{bmatrix} A & 0 \\ 0 & I \end{bmatrix} + \begin{bmatrix} B & 0 \\ 0 & 0 \end{bmatrix} \quad (11)$$

The kinematical equation (10) of the proposed mobile manipulator system is finally derived on velocity-level solution.

3. Optimization of The Kinematic Energy System

As mentioned in Introduction part, a manipulator is redundant when its free joints are more than the minimum number of angles required to execute the special tasks with end-effector. An important issue in operating procedure carries out the inverse motion resolution problem, which is related to the kinematic designing of redundant manipulators. The traditional illustration of such a motion problem is that given the desired trajectory $r_d(t) \in R^m$ of the end-effector of the manipulators, the corresponding trajectory of each joint angle $\theta(t) \in R^n$ is required to be calculated online. In order to get the solution $\theta(t)$, consider the following mathematics:

$$f(\theta) \longrightarrow r_d \quad (12)$$

The kinematical function $f(\cdot)$ is a nonlinear unknown system. Mobile manipulators possess more free joints than the necessity to complete a specific task by the end-effector (in expression $m < n$). Therefore, the repetitive motion scheme for redundant manipulators in literature [7, 9] may not be taken effect for mobile manipulators. In addition, the initial position of each free joint angle has to be considered. For mobile manipulators, wheels of the stationary platform are rotatable and the manipulator upstairs is redundant, which is tended to cause kinematic uncertainty phenomenon. In literature [44], a repeatable motion scheme is proposed for mobile manipulators with two wheels as long as the convergent time is infinity. Motivated by the above research ideas,

we present a repeatable optimization for kinematic energy system with trajectory planning of mobile manipulators. Such an optimization criterion for kinematic control can not only minimize the distance between the initial joints state and the final joints state after executing time, but also reduce the convergent time of each joint angle to zero in limited time.

Let us consider the norm equation (13) for repeatable kinematic energy scheme

$$\begin{aligned} & \text{minimize} \quad \frac{1}{2} \|D\dot{\Theta} + g\|_2^2 \\ & \text{subject to} \quad K\dot{\Theta} = \dot{r}_{wd} + \kappa(r_{wd} - r_w) \end{aligned} \quad (13)$$

where $D = [C, 0; 0, I] \in R^{(n+m) \times (n+m)}$, $C = [A \cos(\theta_0); B]$, $g = [\beta_1 \Psi(\sin(\theta_0) - \sin(\theta_0(0))); \beta_2 \Psi(P_c - P_c(0)); \beta_3 \Psi(\theta - \theta(0))]$. $\theta_0(0)$, $P_c(0)$, and $\theta(0)$ represent the initial state of all free joints including the rotating platform. β_1 , β_2 , β_3 , and κ are four adjustable parameters greater than 0. r_{wd} is the desired path of the end-effector; r_w is the trajectory of end-effector in action. The repetitive optimization of kinematic energy system for mobile manipulator (13) can be simplified as

$$\begin{aligned} & \text{minimize} \quad \frac{1}{2} \dot{\Theta}^T D^T D \dot{\Theta} + g^T \dot{\Theta} \\ & \text{subject to} \quad K\dot{\Theta} = \dot{r}_{wd} + \kappa(r_{wd} - r_w) \end{aligned} \quad (14)$$

3.1. Theoretical Analysis. To realize the repeatable kinematic control for mobile manipulators, there are three important factors in the designing mode, i.e., the each joint angle θ_i of the redundant manipulators located on mobile platform, the rotation direction θ_0 of the platform base, and the location point P_c of the redundant manipulator on the rotational platform. Obviously, three wheels of the mobile platform are likely to deviate from the desired initial position at first. At the same time, joints of the redundant manipulator with seven DOF are prompt to be fixed with incorrect state for the parameter deviation of the manipulator itself. Therefore, repeatable optimization for kinematic energy system with mobile manipulators is equivalent to get the repetitiveness of the three variable θ_i , θ_0 , and P_c . By following the Zhang design rule in [9], we get the following realizing steps.

Firstly, the idea of terminal-time dynamic function $E(t)$ ($E(t) = e_i(t)$), $i=1,2,\dots,n$, can be set up to face finite-time convergent solving problem. Secondly, we can choose a limited value activation function through the Zhang neural network designing rule so that the convergent time of the kinematic energy system is reduced to zero rapidly. We get the dynamic equation of TTZNN as below.

$$\dot{e}_i(t) = -\beta \sqrt{\frac{|e_i(t)|}{1/\delta + |e_i(t)|}} \text{sgn}(e_i(t)) = -\beta \Psi(e_i) \quad (15)$$

with $\beta_i > 0$, $0 < \delta < 1$. $\text{sgn}(\cdot)$ is sign function of the value $-1, 0, 1$. Finally, based on the terminal-time Zhang neural function (15), we expand the designing rule (15) for different

error definition and we obtain the following three types of error functions:

$$E_1 = \sin(\theta_0) - \sin(\theta_0(0)) \quad (16)$$

$$E_2 = P_c - P_c(0) \quad (17)$$

$$E_3 = \theta - \theta(0) \quad (18)$$

where $\theta(0)$, $\theta_0(0)$, and $P_c(0)$ represent the initial position of θ , θ_0 , and P_c . It is necessary to point out that the rotating platform is circulating at 360 degrees with time. The orientational angle θ_0 needs to be returned to the desired initial position. The position error $\theta_0 - \theta_0(0)$ is not possible for realizing repetitive kinematics of the mobile platform. Therefore, the sine function is activated and the disposal scheme of optimization energy system is easy to yield. By combining the design rule (15) of TTZNN, the following three time-varying dynamic equations can be obtained:

$$\dot{\theta}_0 \cos(\theta_0) = -\beta_1 \Psi(\sin(\theta_0) - \sin(\theta_0(0))) \quad (19)$$

$$\dot{P}_c = -\beta_2 \Psi(P_c - P_c(0)) \quad (20)$$

$$\dot{\theta} = -\beta_3 \Psi(\theta - \theta(0)) \quad (21)$$

where $\beta_1 > 0$, $\beta_2 > 0$, and $\beta_3 > 0$ are the scalar parameters for convergent rate. Theoretical analysis in the next section has been proved the equation (19), (20), and (21) holds for $t > t_s$, where t_s shows a constant after e_{ij} converge to zero. Each joint angle of the mobile redundant manipulator system can move back to their desired initial place exponentially no matter the initial position of the mobile manipulator is wherever.

Actually, the important three variables in repeatable kinematic energy system of such mobile manipulator structure are θ_0 , P_c and movable angles Θ . Equations (19)-(20) have to be evolved into matrix form. Let us recall the dynamic equations (1) and (2) in Section 2.1; the following matrix equation can be obtained

$$C\dot{\phi} + \begin{bmatrix} \beta_1 \Psi(\sin(\theta_0) - \sin(\theta_0(0))) \\ \beta_2 \Psi(P_c - P_c(0)) \end{bmatrix} = 0 \quad (22)$$

Then, the matrix-vector time-varying dynamical equation can be described as below:

$$D\dot{\Theta} + g = 0 \quad (23)$$

Combining with the definition of D and g , the corresponding parameters are $D = [C, 0; 0, I]$, $C = [A \cos(\theta_0); B]$, $g = [\beta_1 \Psi(\sin(\theta_0) - \sin(\theta_0(0))); \beta_2 \Psi(P_c - P_c(0)); \beta_3 \Psi(\theta - \theta(0))]$.

Remark 1. From the above derivation, we can get the conclusion that the solution for minimization of the kinematic energy system (14) is equal to solve the time-varying problem (23). The repetitive motion control of such mobile manipulator can be achieved while the convergent time is finite. It is necessary to mention that the kinematic scheme in (14) looks like a traditional optimization matrix equation, but the corresponding parameters of D and K in (14) result in different kinematics meaning. To avoid the occurrence of accidents

during the movement of each joint, it is better to compute the convergent error with $\|D\dot{\Theta} + g\|_2$. $\|\cdot\|_2$ represents a two-norm vector. Therefore, we get the optimization scheme for mobile manipulators for doing repetitive trajectory tasks in finite time not considering the initial position of each kinematic joint.

3.2. Designing for Kinematics Energy System. Analysis about the scheme for kinematics energy system (14) is stated. The optimal index of $\|D\dot{\Theta} + g\|_2^2$ is formulated as $(D\dot{\Theta} + g)^T(D\dot{\Theta} + g)/2$. The optimal performance can be exploited as $X^T D^T D X / 2 + g^T D X + g^T g / 2$. Since the repetitive motion optimization scheme is based on velocity level and the variable $\dot{\Theta}$ is object to be optimized. The term $g^T g / 2$ is thought to be a constant matrix in the executing process. The repeatable optimization index of kinematics energy system can be defined as the following quadratic optimization problem:

$$\begin{aligned} & \text{minimize} \quad \frac{X^T M X}{2} + P^T X \\ & \text{subject to} \quad KX = \dot{r}_{wd} + \kappa(r_{wd} - r_w) \end{aligned} \quad (24)$$

where $X = \dot{\Theta}$, $M = D^T D \in R^{(n+3) \times (n+3)}$, and $P = D^T g \in R^{n+3}$. Other parameters are defined as before. The performance index in (24) is for the repeatable motion planning of kinematics energy system and originated from the simplified formula of (13) and (14). The term of $KX = \dot{r}_{wd} + \kappa(r_{wd} - r_w)$ represents forward kinematics equation while the initial moving point is drifting from the desired path.

Remark 2. Let us look at the criterion (24); the kinematic scheme with equation limitation has not been considered joint limits of the redundant manipulator on mobile platform. Accidents may be happened while the unexpected trajectories are given and the redundant manipulators may be damaged, which leads to do nonrepeated motion. At the same time, we can not incorporate the physical limits of the redundant manipulators into the optimization scheme. Therefore, we set the maximum border of each angle joint in programming before simulation experiments are performed. The primary tasks will be completed accurately with this three-wheel manipulator system.

4. Terminal-Time ZNN Approach

In Section 3, a universal repeatable optimization of the kinematic energy system is presented and formulated for trajectory planning of mobile manipulators with three wheels. To solve the optimal scheme (24), we use the solution of terminal-time Zhang neural network (TTZNN) approach (15) to calculate the convergent time t . By deriving the variable $\dot{\Theta}$ with Lagrangian theory, we get the following time-varying equation:

$$W(t) y(t) - v(t) = 0 \quad (25)$$

with $W(t) = [M, K^T(t); K(t), 0] \in R^{(n+m) \times (n+m)}$, $y(t) = [X(t); \lambda(t)] \in R^{n+m}$, and $v(t) = [-P; \dot{r}_{wd} + \kappa(r_{wd} - r_w)]$.

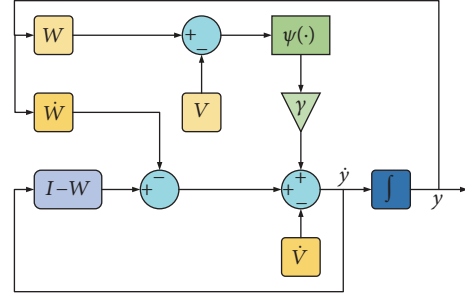


FIGURE 3: Diagram procedure of the TTZNN model (27).

The vector-valued convergent error function is given as

$$E(t) = W(t) y(t) - v(t) \quad (26)$$

To make the every vector $e_i(t)$ of convergent error to zero timely, following the TTZNN design formula (15), the repetitive kinematics modeling based on TTZNN can be depicted:

$$\dot{y} = (I - W) \dot{y} + \dot{v} - \dot{W} y - \beta \Psi(Wy - v) \quad (27)$$

The corresponding control diagram for TTZNN (27) is visualized in Figure 3.

Theorem 3. Consider the repeatable kinematics scheme (24). Given any initial value of vector $y(0)$ in (27), the state value $y(t)$ of dynamic system (27) globally converges to the theoretical value $y^*(t)$ in finite time t_s :

$$\begin{aligned} t_s \leq & \frac{1}{\beta \delta} \left(\frac{H^3(e_i(0))}{\delta e_i(0)} - H(e_i(0)) \right. \\ & \left. - \frac{1}{2} \ln \left| \frac{H(e_i(0)) - 1}{H(e_i(0)) + 1} \right| \right) \end{aligned} \quad (28)$$

where $H(e_i(0)) = \sqrt{1 + (\delta e_i(0))^{-1}}$.

Proof. The proof procedure is divided to two parts. Firstly, to prove the stability of the proposed TTZNN, we need to introduce the Lyapunov theorem candidate like $V(t) = e_i^2(t)/2$. The time derivative of $V(t)$ is expressed $\dot{V}(t) = e_i \dot{e}_i$. Therefore, we can get the equation

$$\dot{V}(t) = -\beta \sqrt{\frac{|e_i(t)|}{1/\delta + |e_i(t)|}} \text{sgn}(e_i(t)) e_{ij}(t) \quad (29)$$

where $\beta > 0$, $\dot{V}(t) < 0$. $y(t)$ in TTZNN modeling (27) can converge to its theoretical value $y^*(t)$.

Secondly, let us consider the terminal-time dynamic system (15); if $e_i(t) \geq 0$, we get

$$\dot{e}_i(t) = -\beta \sqrt{\frac{e_i(t)}{\delta^{-1} + e_i(t)}} \quad (30)$$

In order to solve (30) with time t , we need to introduce symbol x , which satisfies $e_{ij} = (\delta x)^{-1}$. Then, we get

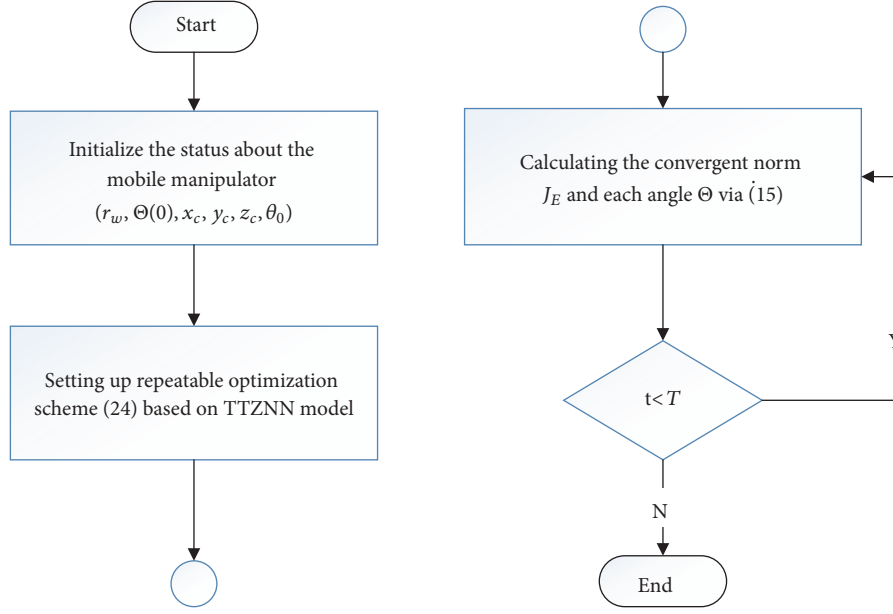


FIGURE 4: The flowchart of TTZNN model for kinematic planning of the mobile manipulator.

$dt = \sqrt{1+x}(\beta\delta x^2)^{-1}dx$. By means of integral methods, we obtain the solution of (30):

$$t = \frac{-1}{\beta\delta} \left[\frac{(1+x)^{3/2}}{x} - \frac{1}{2} \left(2\sqrt{1+x} + \ln \left| \frac{\sqrt{1+x}-1}{\sqrt{1+x}+1} \right| \right) \right] \Bigg|_{x(0)}^{x(t)} \quad (31)$$

Setting $x = (\delta e_i)^{-1}$, we have

$$t = \frac{-1}{\beta\delta} \left(\frac{H^3(e_i)}{(\delta e_i)^{-1}} - H(e_i) - \frac{1}{2} \ln \left| \frac{H(e_i)-1}{H(e_i)+1} \right| \right) \Bigg|_{x(0)}^{x(t)} \quad (32)$$

When $e_i(t) = 0$, the convergence time is calculated.

$$t_s \leq \frac{1}{\beta\delta} \left(\frac{H^3(e_i(0))}{(\delta e_i(0))^{-1}} - H(e_i(0)) - \frac{1}{2} \ln \left| \frac{H(e_i(0))-1}{H(e_i(0))+1} \right| \right) \quad (33)$$

□

For better understanding, the solution steps for the entire executing process of kinematics energy optimization algorithm are visualized in Figure 4.

5. Verification for Optimization of Kinematic Energy System

In this section, different trajectories with the three-wheel mobile manipulator visualized in Figure 1 are performed to

illustrate the repetitiveness and finiteness of the proposed optimization scheme of the kinematics system based on TTZNN model (27). Comparisons among ZNN model, TTZNN model, and GNN model are analyzed from the perspective of convergence in form of $\|\cdot\|_2$. It is necessary to point out that the scalar parameters β , λ , κ , and δ are positive constant. In the executing procedure of mobile manipulators, the parameters β and λ are inappropriate to be set much larger as the hardware is not allowed. It will bring algebraic circles with simulation experiments and lead to termination of the mobile manipulator in motion.

5.1. Circular Path Tracking. To realize the repeatable kinematics of the proposed mobile manipulator model, the end-effector is required to complete a circular path with radius $r = 0.5\text{m}$. During the tracking procedure, the desired initial joints of the redundant manipulator PA10 are $\theta^*(0) = [0, -\pi/4, 0, \pi/2, 0, -\pi/4, 0]^T$. Joints of the three rotational wheels are $\varphi = [0, 0, 0]$. The actual initial joints are $\theta(0) = [0, -\pi/4, 0, \pi/2, 0, -\pi/4 + 2, 0]^T$. The deviation of the sixth angle with redundant manipulator is 2 rad. The executing recurrent time is $T = 10\text{s}$. The axes of X, Y, Z for the desired trajectory of the end-effector are given as

$$\begin{aligned} r_{\text{wdx}}(t) &= 0.2 \times \cos \left(2\pi \left(\sin \left(\frac{\pi t}{2T} \right) \right)^2 \right) - 0.1646 \\ r_{\text{wdy}}(t) &= 0.15 \times \cos \left(\frac{\pi}{6} \right) \sin \left(2\pi \left(\sin \left(\frac{\pi t}{2T} \right) \right)^2 \right) \\ r_{\text{wdz}}(t) &= 0.1 \times \cos \left(2\pi \left(\sin \left(\frac{\pi t}{2T} \right) \right)^2 \right) + 0.5518 \end{aligned} \quad (34)$$

The corresponding simulation results are visualized in Figures 5, 6, and 7. Figure 5(a) shows the motion trajectory

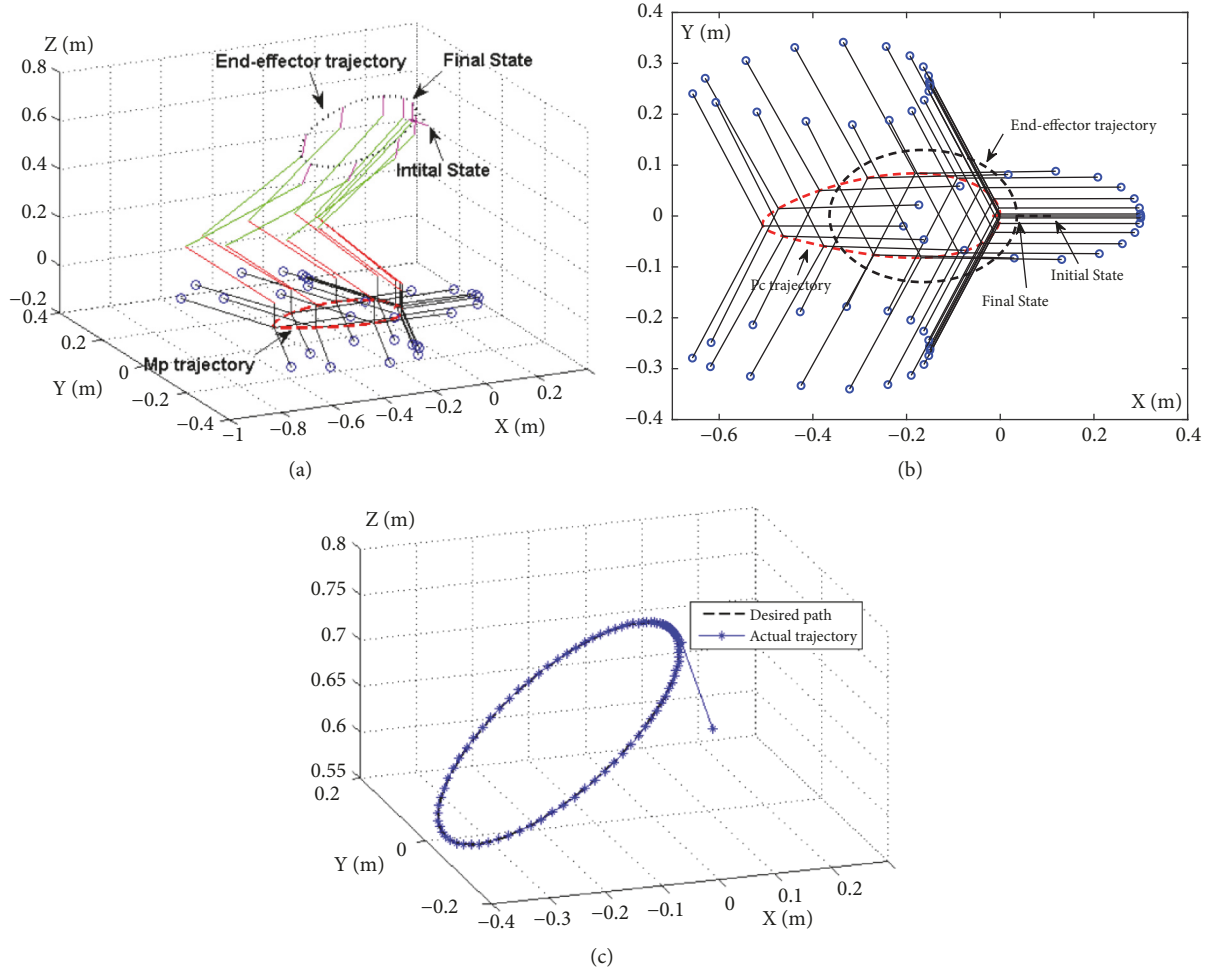


FIGURE 5: Simulation results about repeatable optimization of kinematic energy system with TTZNN solver when the end-effector is required to complete a circular path. (a) Motion trajectories with the entire mobile manipulator. (b) Vertical view for entire mobile manipulator. (c) Profiles of the desired trajectory and actual path of the end-effector.

of the entire mobile manipulator with ten free joints during the executing time. The actual path of the end-effector and the desired path of the end-effector are overlapped, which illustrates the kinematic repetitiveness. Figure 5(b) shows us the kinematic trajectories of the platform wheels, connection point C, and end-effector from vertical perspective. The motion direction of the end-effector of the redundant manipulator is visualized in Figure 5(c). The initial position of the end-effector is deviate from the desired trajectory at first. Then, it moves to the desired trajectory in few seconds. The corresponding convergent precision is specialized in Figures 6(b) and 6(a). The distance between the desired path and actual motion path is less than 10^{-4} in X, Y, Z three directions. The joints movements with the redundant manipulator depicted in Figure 7(a) are continuous and smooth, which illustrates the all the joints come back to the initial desired position.

For illustrating the movement of three wheels with mobile platform, Figures 6(c), 6(d), 7(b), and 7(c) are investigated to illustrate the final position of the mobile wheels. At the

beginning of the task, profiles of mobile platform ($x_c(0) = 0, y_c(0) = 0, z_c(0) = 0$) are specialized in Figure 7(b). Later, the mobile platform moves with the redundant manipulator quickly to complete the circular path. It is to say that the flexible platform takes larger kinematic space than fixed base manipulators. The change profile of the heading angle with the mobile platform θ_0 is shown in Figure 6(d), which coordinates with the rotation base. Figure 7(c) visualizes the trajectories of three wheels. At first, the three Swedish wheels are stationary. With increase of radius, the mobile base needs to help the redundant manipulator for tracking. Therefore, it moves away from the initial point $x_c(0), y_c(0), \theta_0(0)$ gradually but returns back to the desired space at last, which is synthesized with the profiles in Figures 6(c) and 6(d). The above experimental results substantiate the effectiveness of the proposed repeatable kinematic optimization (24) based on TTZNN neural solver.

5.2. Lissajous Path Tracking. To verify the finiteness and convergence of the proposed TTZNN method, we outline a

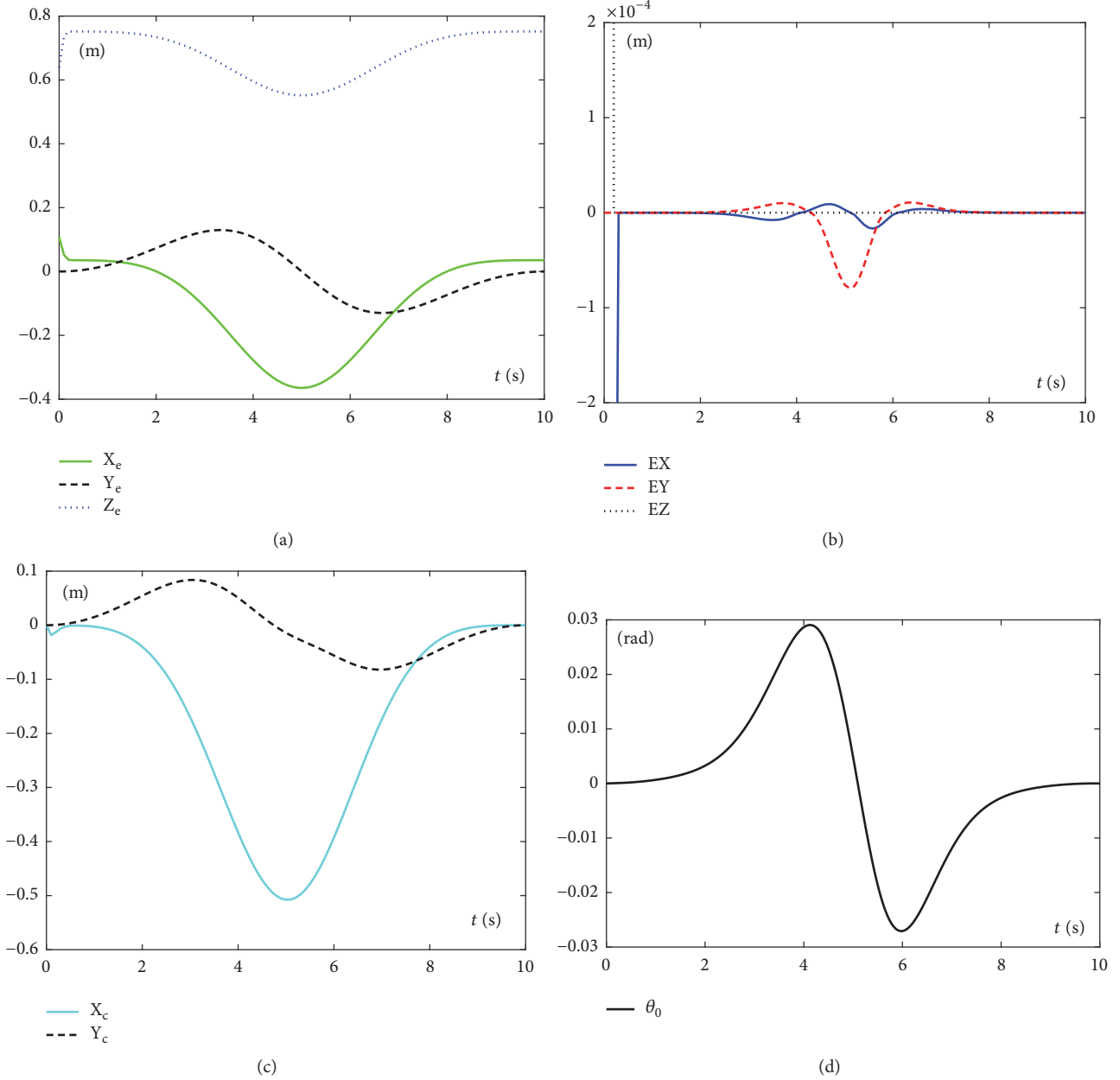


FIGURE 6: Circular planning profiles of the three-wheel mobile manipulator synthesized by TTZNN model (27). (a) Position files of the end-effector. (b) Position error of the end-effector in three dimensions. (c) Profiles of the mobile base for P_C . (d) Trajectory with heading angle θ_0 .

desired Lissajous-shaped trajectory to be functioned by the end-effector of the mobile manipulator in three axis x , y , and z .

$$\begin{aligned}
 r_{\text{wdx}}(t) &= 0.8 \cos \left(4\pi \left(\sin \left(\frac{\pi t}{2T} \right) \right)^2 + \frac{\pi}{6} \right) - 0.7645 \\
 r_{\text{wdy}}(t) &= 0.8 \sin \left(4\pi \left(\sin \left(\frac{\pi t}{2T} \right) \right)^2 + \frac{\pi}{6} \right) - 0.0073 \\
 r_{\text{wdz}}(t) &= 0.7518
 \end{aligned} \quad (35)$$

The executing recurrent time is $T = 10$ s. The designing parameters $\beta_1 = 10$, $\beta_2 = 10$ and $\beta_3 = 10$ are used in this manuscript. The initial desired position of the mobile base is set $x_c = 0$, $y_c = 0$, $z_c = 0$. The initial value of joint angles with redundant manipulator PA10 is given $\theta^*(0) = [0, -\pi/4, 0, \pi/2, 0, -\pi/4, 0]^T$ rad. Deviation angle with the sixth joint of redundant manipulator PA10 is 2 rad.

The corresponding experimental results are shown in Figures 8–10 by the solution of TTZNN model (15) when the end-effector of the mobile manipulator is given to complete

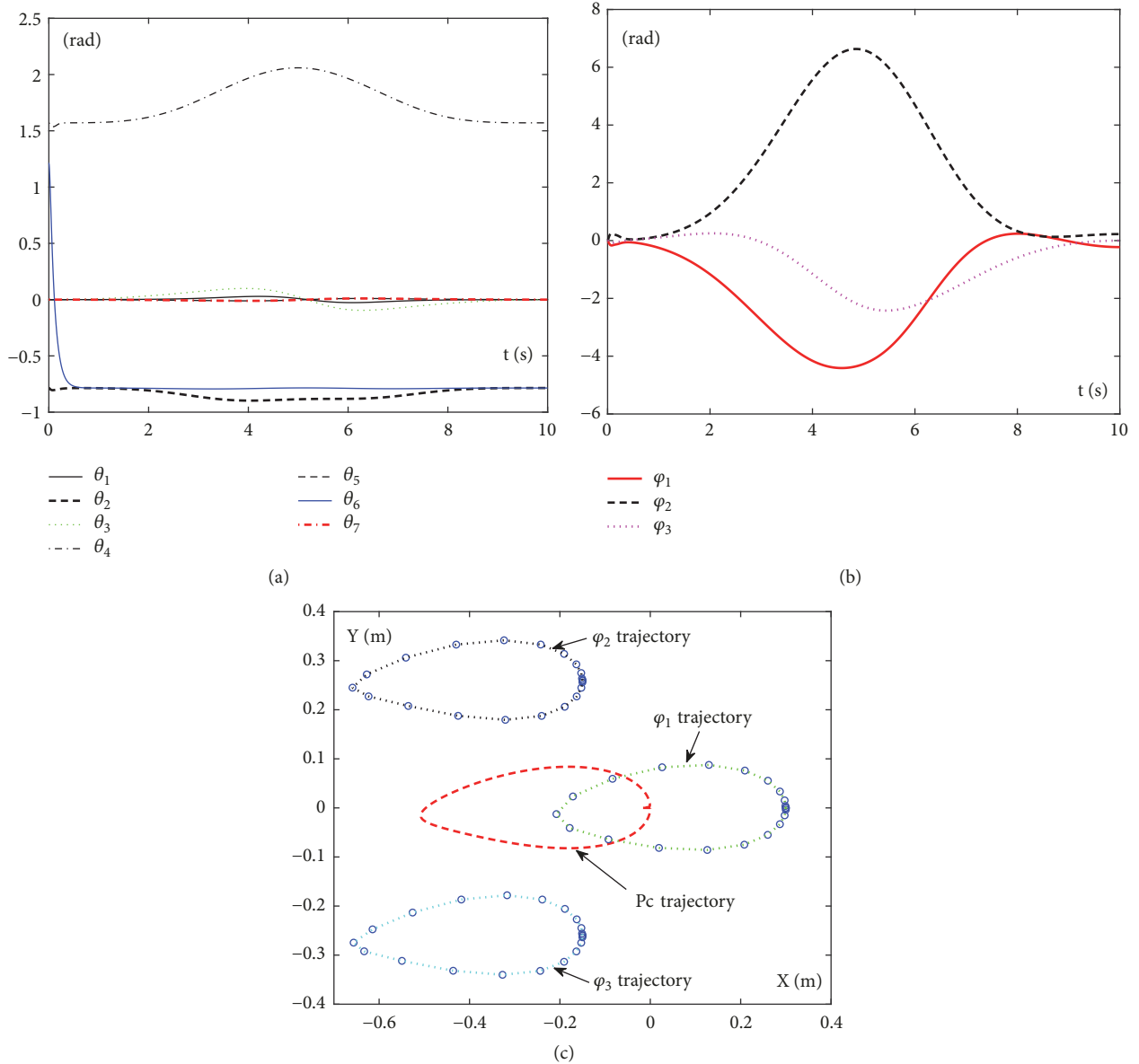


FIGURE 7: Profiles about the free joint angles of the mobile manipulator. (a) Motion trajectories of each joint angle of redundant manipulator PA10. (b) Rotating profiles for three wheels. (c) Motion trajectories with the mobile base.

the Lissajous-shaped path. Figure 8(a) shows that the desired trajectory and the actual motion path are coincide well with each other. From Figure 8(c), we can see the line with “+” symbol is not at the desired path at first and move near to the solid line in a few seconds. In Figure 8(b), two lines are overlapped in kinematic procedure. Figure 9(b) depicts the profiles of the position error E_x, E_y, E_z of the end-effector. The precision of position error in three dimensions is less than 10^{-4} , which is consistent with the theoretical analysis in Section 3.2. More simulation results about the kinematics of mobile manipulator are visualized in Figures 9(a) and 9(c). Obviously, each joint is smooth and regular. Furthermore, to verify the repetitive ness of the proposed kinematic optimization scheme (24) with the movable base, movements

of the mobile platform with three wheels are illustrated in Figure 10. The details of the kinematic three wheels are shown in Figure 10(c). Pay attention to the statement of the three wheels. They are stationary during 1s. From $t = 1$ s, three wheels begin to move away and reach 0.6m in five seconds. From $t = 5$ s, three wheels move towards to the desired initial position, which can be seen in Figure 10(b). Because the Lissajous-shaped path can be reached by the redundant manipulator at the beginning, with the extension of kinematic path, the mobile base carrying the redundant manipulator moves together and returns to the desired initial position ($x_c(0) = 0, y_c(0) = 0$ and $\theta_0(0) = 0$) in the end, which is well displayed in Figures 10(a) and 10(d). All the free joints θ_i of the redundant manipulator PA10 return to their

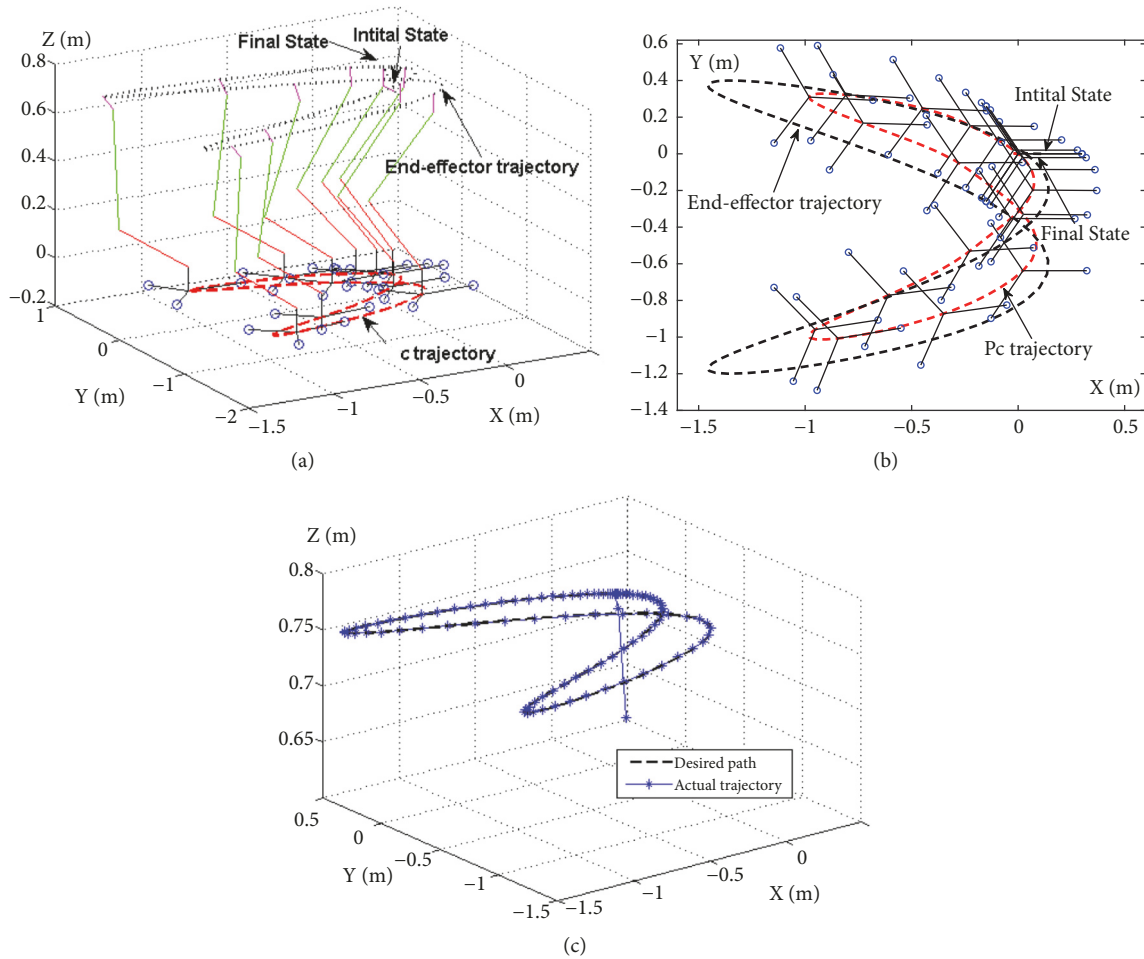


FIGURE 8: Lissajous path tracking profiles synthesized by TTZNN model (27). (a) Trajectories for the mobile manipulator. (b) Vertical view for the three-wheel mobile manipulator. (c) Lissajous tracking profiles of the end-effector.

desired state $\theta^*(0)$. The above simulation examples are fully verified the effectiveness of the repeatable motion planning by TTZNN model solution.

5.3. Comparisons with Existing Kinematic Energy Optimization. To witness the finiteness and precision of the proposed repeatable motion scheme with TTZNN model (15), the comparisons with the existed repetitive motion solutions (GNN, ZNN, and TTZNN) are simulated in the following part.

(1) *Comparison with the Scheme of Gradient Neural Network (GNN) [26].* One kind of recurrent neural network models is Gradient neural network (GNN). It is an alternative for solving time-varying problems and is applied to kinematic planning of manipulators. The dynamic formula with GNN can be shown in (36):

$$\dot{y}(t) = -\gamma W^T(t)(W(t)y(t) - v(t)) \quad (36)$$

where $\gamma > 0$ is the adjustable parameter to scale the convergent speed. Linear activation function is considered. In the whole experimental process, $\gamma = 1$ is set. The repeatable motion plan is the same as (37). The simulation examples are

shown in Figure 11(a) synthesized with GNN model when the end-effector of the mobile manipulator is assigned to execute a circle trajectory. Obviously, the motion trajectory of the end-effector is not coincided with the desired trajectory even after the execution time, which is visualized in Figure 11(a). Then convergent error of position XYZ axis with the end-effector takes larger value, which is a good explanation of the phenomenon in Figure 11(c). Comparing with the ZNN model for repetitive scheme in (24), GNN model does not possess the ability for time-varying inverse kinematics even the scalar parameters γ are set 10^4 .

The above simulation profiles illustrate that GNN model is not effective for dealing time-varying problems. Simultaneous kinematics of the movable platform and the flexible manipulator makes the tracking tasks difficult within fixed time.

(2) *Comparison with the Scheme of Zhang Neural Network (ZNN) [9].* Another kind of the recurrent neural network models is ZNN, which is designated to address time-varying problems. The convergent error of dynamic kinematic equation can rapidly reduce to zero as long as time is infinite. Motivated by the theorem of ZNN, a repetitive motion plan

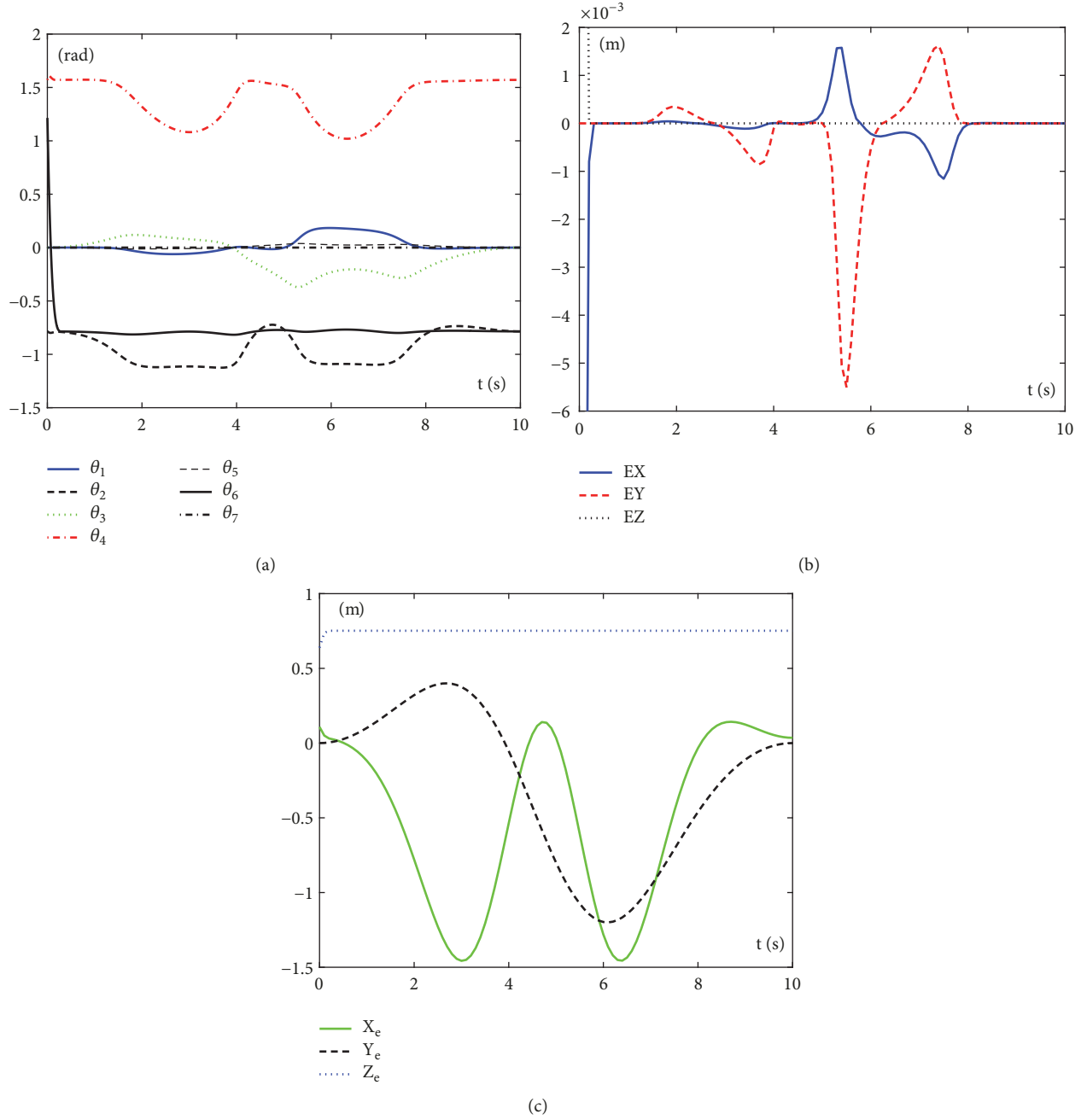


FIGURE 9: Simulated programs for the repeatable optimization of kinematic energy system (24) under the control of TTZNN. (a) Joints files. (b) Position error of the end-effector (c) Position changing profiles about the end-effector.

for redundant manipulators is set as: minimize $\dot{\theta}^T \dot{\theta} / 2 + u(\theta(t) - \theta(0))^T \dot{\theta}$, subject to $J(\theta)\dot{\theta} = \dot{r} + \kappa(r - f(\theta))$. The ZNN model is defined as

$$\begin{aligned} \dot{y}(t) = & -\dot{W}(t)y(t) + (I - W(t))\dot{y}(t) + \dot{v}(t) \\ & + \gamma[W(t)y(t) - v(t)] \end{aligned} \quad (37)$$

where $\gamma > 0$ is used to scale the convergent rate. For comparisons, the scaling parameter $\gamma = 1$ is set. The corresponding profiles synthesized by ZNN (37) are visualized in Figures 11(b) and 11(d) when a circle tracking path is set. As seen

from Figure 11(b), considering the deviation of the initial position, each joint of the mobile manipulator comes back to the desired place finally. The position error of E_x, E_y, E_z reaches 10^{-4} in Figure 11(d). After the motion task, the mobile manipulator has returned to the desired position as long as time goes infinity. To verify the convergence speed of three different neural network model (GNN, ZNN, and TTZNN), the residual error $J_E = \|W(t)y(t) - v(t)\|_2$ is supposed to show the different convergent rate when the end-effector is required to perform a circular path. In Figure 12, the blue trajectory (with TTZNN) sharply reduces to zero within

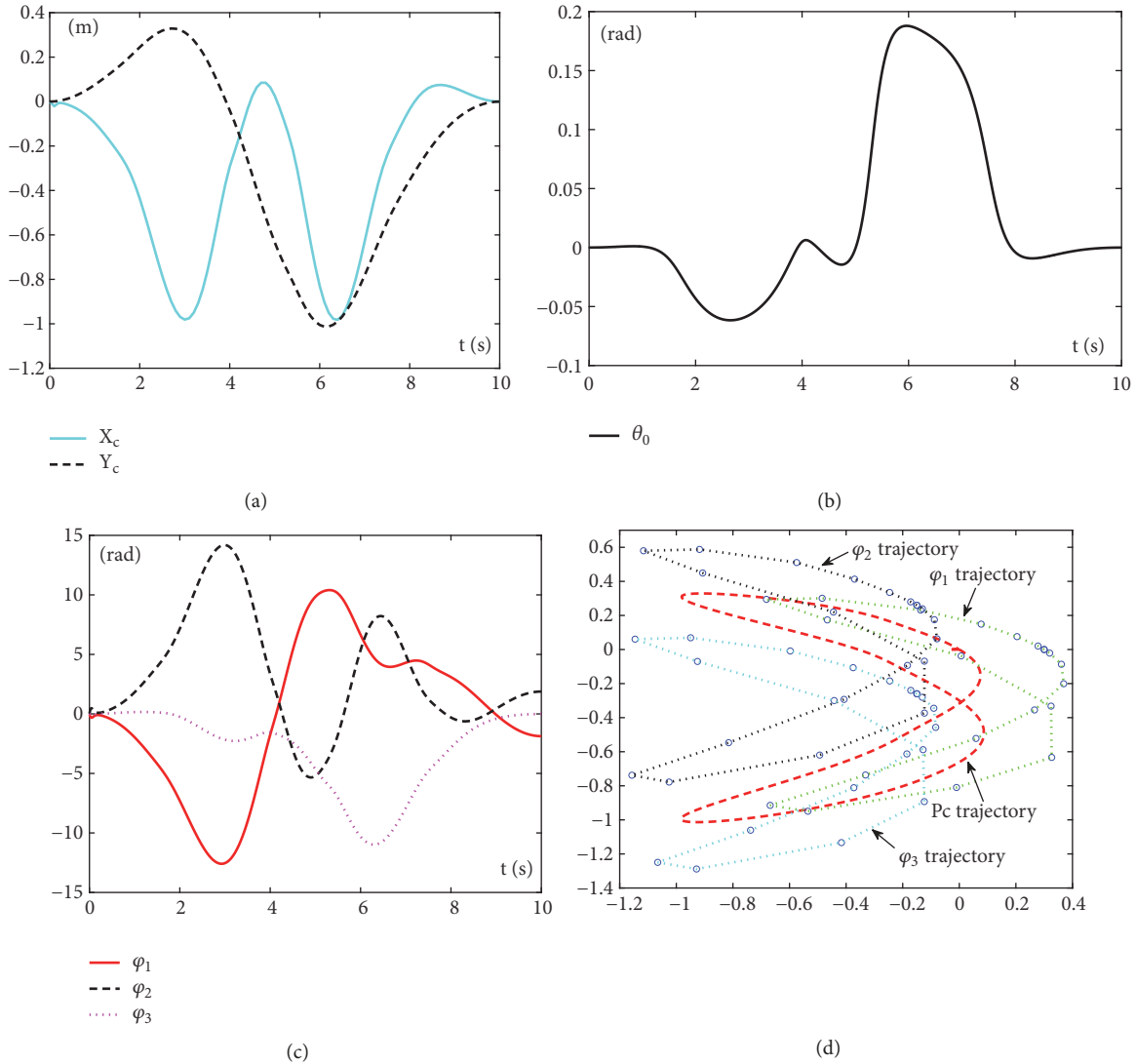


FIGURE 10: Simulated information about the mobile platform. (a) Position files of the mobile base. (b) Heading angle profiles. (c) Rotating profiles for three wheels. (d) Movable platform trajectories.

0.05s, while the red dotted line shows comparatively slower speed. The residual error with GNN in red color decreases very slow and even does not reach zero at $t = 10$ s.

To show the different convergent precision with GNN, ZNN, and TTZNN, Table 3 lists the displacement of each joint with the proposed mobile manipulator model. From Table 3, under the repeatable optimization scheme in (24) with the solution of ZNN, the convergent precision displayed is less than 10^{-5} rad. The maximum joint distance with GNN is 0.1. When the repeatable optimization of kinematics system with TTZNN is operated, distance between desired position and initial position is around 10^{-8} , which can be seen in Table 3. Table 2 shows us the kinematic profiles of the mobile platform with three position parameters x_c, y_c, θ_0 . From Table 2, under the repeatable motion planning (24) with GNN solver, x_c, y_c, θ_0 do not return to their initial position. On the contrary, with TTZNN and ZNN, the movable base has returned to the initial position in 10s. We

TABLE 2: Position profiles of the mobile base when its end-effector tracks a circle path using different neural models.

Variate	Scheme	$t = 0$	$t = 10$ s	Position error
x_c (m)	GNN	0	0.081125	0.081125
	ZNN	0	-9.06238e-05	9.06238e-05
	TTZNN	0	-4.85327e-09	4.85327e-09
y_c (m)	GNN	0	-0.050597	0.050597
	ZNN	0	1.37810e-05	1.37810e-05
	TTZNN	0	7.45148e-09	7.45148e-09
θ_0 (rad)	GNN	0	-0.169099	0.169099
	ZNN	0	-1.67426e-06	1.67426e-06
	TTZNN	0	4.97184e-09	4.97184e-09

can see the convergent precision has reached to 10^{-9} , while the corresponding position parameters x_c, y_c and θ_0 with

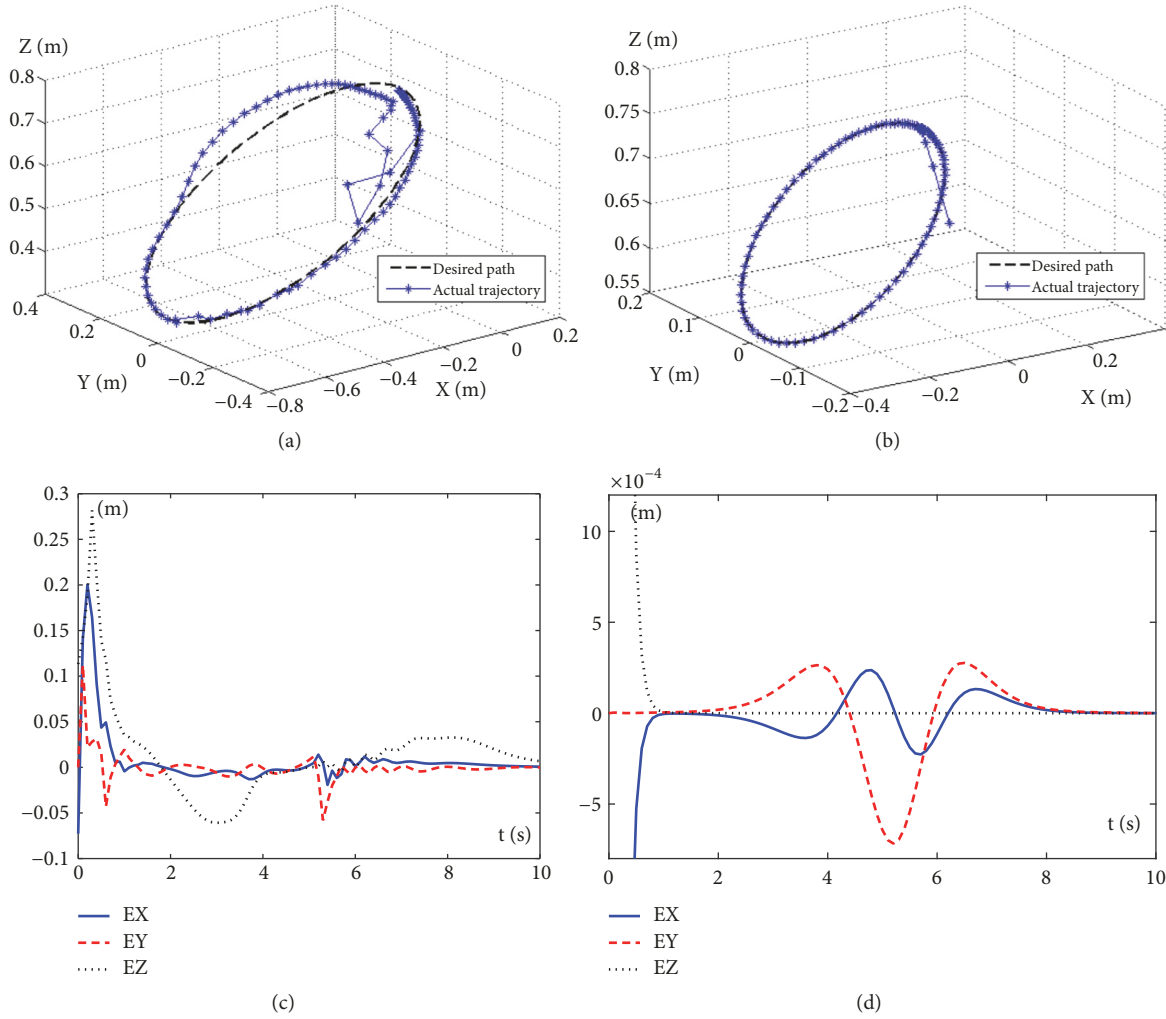


FIGURE 11: Comparison profiles using different neural optimization scheme. (a) Trajectories of the end-effector with GNN. (b) Trajectories of the end-effector with ZNN. (c) Position error of the end-effector with GNN. (d) Position error of the end-effector with ZNN.

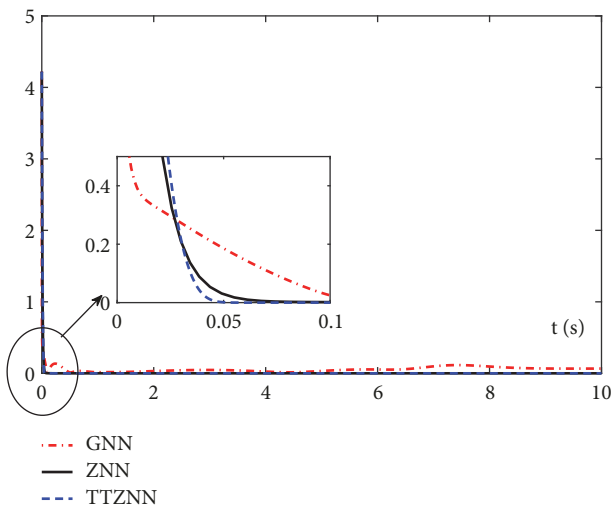


FIGURE 12: Residual error J_E with different neural networks under the kinematic repeatable scheme (24).

ZNN are less than 10^{-5} . It is necessary to state that the ZNN model can do better performance in trajectory planning of mobile manipulators when the adjusting parameter is more than $\gamma = 1000$. Though better experimental results can be obtained as the same results performed by TTZNN, the convergent time is infinite, which is not prompt to be applied in engineering fields.

6. Conclusion

To achieve the finite-time convergence for repetitive trajectory planning of mobile manipulators, an optimization scheme of kinematic energy system based on TTZNN is presented and analyzed. Theoretical finite time has been proved and the upper limitation of the convergent time has been calculated for the formulation of repeatable optimization scheme. A mobile platform of three wheels and a redundant manipulator of seven free joints are combined together to constitute a new mobile manipulator system.

TABLE 3: Free joints of the manipulator PA10 synthesized with scheme (24) with different neural solutions

Joint (rad)	Scheme	$\theta_i^*(0)$	$\theta_i(10)$	$ \theta_i(10) - \theta_i^*(0) $
θ_1	GNN	0	-0.001243	0.001243
	ZNN	0	-4.98251e-05	4.98251e-05
	TTZNN	0	-5.21435e-09	5.21435e-09
θ_2	GNN	-0.785398	-0.886456	0.101058
	ZNN	-0.785398	-0.785275	1.23249e-04
	TTZNN	-0.785398	-0.785398	5.84480e-09
θ_3	GNN	0	0.087746	0.087746
	ZNN	0	-5.58358e-05	5.58358e-05
	TTZNN	0	-1.30718e-08	1.30718e-08
θ_4	GNN	1.57080	1.56293	0.007871
	ZNN	1.57080	1.57078	1.18503e-05
	TTZNN	1.57080	1.57080	5.74257e-10
θ_5	GNN	0	-0.009014	0.009014
	ZNN	0	6.14588e-06	6.14588e-06
	TTZNN	0	1.21890e-09	1.21890e-09
θ_6	GNN	1.21460	-0.796231	0.010832
	ZNN	1.21460	-0.785364	3.41855e-05
	TTZNN	1.21460	-0.785398	8.99498e-09
θ_7	GNN	0	0	0
	ZNN	0	0	0
	TTZNN	0	0	0

Numerical simulations via the proposed mobile manipulator fully substantiate the effectiveness of the optimization method for any initial joint position. Future work may focus on the realization for resisting disturbance of noise pollution when such a mobile manipulator is assigned to do repeatable work.

Data Availability

The source code and source data can be provided by contacting with the corresponding author.

Conflicts of Interest

The authors declare that there are no conflicts of interest regarding the publication of this paper.

Acknowledgments

This study was partly supported by National Natural Science Foundation of China (nos. 61771193, 61803338, and 61703183) and Public Projects of Zhejiang Province (LGG18F020011 and LGG19F030010).

References

[1] W. He, W. Ge, Y. Li, Y.-J. Liu, C. Yang, and C. Sun, "Model identification and control design for a humanoid robot," *IEEE Transactions on Systems, Man, and Cybernetics: Systems*, vol. 47, no. 1, pp. 45–57, 2017.

[2] Q. Chen, X. Ren, and J. Na, "Adaptive finite-time neural control of servo systems with non-linear dead-zone," *Neural Computing and Applications*, vol. 28, no. 2, pp. 3725–3736, 2017.

[3] J. Na, Z. Yang, S. Kamal, and L. Hu, "Bio-inspired learning and adaptation for optimization and control of complex systems," *Complexity*, vol. 2019, Article ID 9325364, 3 pages, 2019.

[4] Q. Chen, S. Xie, M. Sun, and X. He, "Adaptive non-singular fixed-time attitude stabilization of uncertain spacecraft," *IEEE Transactions on Aerospace and Electronic Systems*, vol. 54, no. 6, pp. 2937–2950, 2018.

[5] Y. Jiang, Y. Xu, and Y. Liu, "Performance evaluation of feature detection and matching in stereo visual odometry," *Neurocomputing*, vol. 120, pp. 380–390, 2013.

[6] F. Zhang, X. Liao, and G. Zhang, "Qualitative behavior of the Lorenz-like chaotic system describing the flow between two concentric rotating spheres," *Complexity*, vol. 21, no. S2, pp. 67–72, 2016.

[7] Z. Zhang and Y. Zhang, "Variable joint-velocity limits of redundant robot manipulators handled by quadratic programming," *IEEE/ASME Transactions on Mechatronics*, vol. 18, no. 2, pp. 674–686, 2013.

[8] L. Jin and Y. Zhang, "G2-Type SRMPC scheme for synchronous manipulation of two redundant robot arms," *IEEE Transactions on Cybernetics*, vol. 45, no. 2, pp. 153–164, 2015.

[9] Y. Zhang, Z. Tan, K. Chen, Z. Yang, and X. Lv, "Repetitive motion of redundant robots planned by three kinds of recurrent neural networks and illustrated with a four-link planar manipulator's straight-line example," *Robotics and Autonomous Systems*, vol. 57, no. 6-7, pp. 645–651, 2009.

[10] E. Maulana, M. A. Muslim, and A. Zainuri, "Inverse kinematics of a two-wheeled differential drive an autonomous mobile robot," in *Proceedings of the 2014 Electrical Power, Electronics, Communications, Controls and Informatics Seminar (EECCIS)*, pp. 93–98, Malang, Indonesia, August 2014.

[11] Q. Jiang and V. Kumar, "The inverse kinematics of cooperative transport with multiple aerial robots," *IEEE Transactions on Robotics*, vol. 29, no. 1, pp. 136–145, 2013.

[12] J. S. Kim, Y. H. Jeong, and J. H. Park, "A geometric approach for forward kinematics analysis of a 3-SPS/S redundant motion manipulator with an extra sensor using conformal geometric algebra," *Meccanica*, vol. 51, no. 10, pp. 2289–2304, 2016.

[13] K. Tchon, "Repeatability of inverse kinematics algorithms for mobile manipulators," *IEEE Transactions on Automatic Control*, vol. 47, no. 8, pp. 1376–1380, 2002.

[14] M. S. Miah and W. Gueaieb, "RFID-based mobile robot trajectory tracking and point stabilization through on-line neighboring optimal control," *Journal of Intelligent & Robotic Systems*, vol. 78, no. 3-4, pp. 377–399, 2015.

[15] M. Tao, Q. Chen, X. He, and M. Sun, "Adaptive fixed-time fault-tolerant control for rigid spacecraft using a double power reaching law," *International Journal of Robust and Nonlinear Control*, vol. 29, no. 12, pp. 4022–4040, 2019.

[16] C. Lian, X. Xu, H. Chen, and H. He, "Near-optimal tracking control of mobile robots via receding-horizon dual heuristic programming," *IEEE Transactions on Cybernetics*, vol. 46, no. 11, pp. 2484–2496, 2016.

[17] D. Xu, D. Zhao, J. Yi, and X. Tan, "Trajectory tracking control of omnidirectional wheeled mobile manipulators: robust neural network-based sliding mode approach," *IEEE Transactions on Systems, Man & Cybernetics, Part B: Cybernetics*, vol. 39, no. 3, pp. 788–799, 2009.

- [18] G. Franzè and W. Lucia, "An obstacle avoidance model predictive control scheme for mobile robots subject to nonholonomic constraints: A sum-of-squares approach," *Journal of The Franklin Institute*, vol. 352, no. 6, pp. 2358–2380, 2015.
- [19] M. Rolf and J. Steil, "Efficient exploratory learning of inverse kinematics on a bionic elephant trunk," *IEEE Transactions on Neural Networks and Learning Systems*, vol. 25, no. 6, pp. 1147–1160, 2014.
- [20] L. Xiao and Y. Zhang, "Solving time-varying inverse kinematics problem of wheeled mobile manipulators using Zhang neural network with exponential convergence," *Nonlinear Dynamics*, vol. 76, no. 2, pp. 1543–1559, 2014.
- [21] W. He, S. Ge, and Y. Li, "Neural network control of a rehabilitation robot by state and output feedback," *Journal of Intelligent and Robotic Systems*, vol. 80, no. 1, pp. 15–31, 2015.
- [22] Q. Chen, L. Shi, J. Na, X. Ren, and Y. Nan, "Adaptive echo state network control for a class of pure-feedback systems with input and output constraints," *Neurocomputing*, vol. 275, pp. 1370–1382, 2018.
- [23] J. Na, Q. Chen, X. Ren, and Y. Guo, "Adaptive prescribed performance motion control of servo mechanisms with friction compensation," *IEEE Transactions on Industrial Electronics*, vol. 61, no. 1, pp. 486–494, 2014.
- [24] W. He and Y. Dong, "Adaptive fuzzy neural network control for a constrained robot using impedance learning," *IEEE Transactions on Neural Networks and Learning Systems*, vol. 29, no. 4, pp. 1174–1186, 2018.
- [25] P. V. Cuong and W. Y. Nan, "Adaptive trajectory tracking neural network control with robust compensator for robot manipulators," *Neural Computing and Applications*, vol. 27, no. 2, pp. 525–536, 2016.
- [26] B. Huang and C. Ma, "Gradient-based iterative algorithms for generalized coupled Sylvester-conjugate matrix equations," *Computers & Mathematics with Applications*, vol. 75, no. 7, pp. 169–179, 2018.
- [27] D. Chen, Y. Zhang, and S. Li, "Tracking Control of Robot Manipulators with Unknown Models: A Jacobian-Matrix-Adaptation Method," *IEEE Transactions on Industrial Informatics*, vol. 14, no. 7, pp. 3044–3053, 2018.
- [28] Y. Wang, L. Cheng, Z.-G. Hou, J. Yu, and M. Tan, "Optimal formation of multirobot systems based on a recurrent neural network," *IEEE Transactions on Neural Networks and Learning Systems*, vol. 27, no. 2, pp. 322–333, 2016.
- [29] S. Li, J. He, and Y. Li, "Distributed recurrent neural networks for cooperative control of manipulators: a game-theoretic perspective," *IEEE Transactions on Neural Networks and Learning Systems*, vol. 28, no. 2, pp. 415–426, 2017.
- [30] L. Jin, S. Li, L. Xiao, R. Lu, and B. Liao, "Cooperative motion generation in a distributed network of redundant robot manipulators with noises," *IEEE Transactions on Systems, Man, and Cybernetics: Systems*, vol. 99, no. 1, pp. 217–227, 2017.
- [31] Z. Zhang, Y. Lu, L. Zheng, S. Li, Z. Yu, and Y. Li, "A new varying-parameter convergent-differential neural-network for solving time-varying convex QP problem constrained by linearequality," *IEEE Transactions on Automatic Control*, vol. 63, no. 12, pp. 4110–4125, 2018.
- [32] Z. Zhang, L. Zheng, J. Weng, Y. Mao, W. Lu, and L. Xiao, "A new varying-parameter recurrent neural-network for online solution of time-varying sylvester equation," *IEEE Transactions on Cybernetics*, vol. 48, no. 11, pp. 3135–3148, 2018.
- [33] Y. Zhang, Z. Xiao, D. Guo, and M. Miao, "Singularity-conquering tracking control of a class of chaotic systems using Zhang-gradient dynamics," *IET Control Theory & Applications*, vol. 9, no. 6, pp. 871–881, 2015.
- [34] Y. Zhang, W. Li, and Z. Zhang, "Physical-limits-constrained minimum velocity norm coordinating scheme for wheeled mobile redundant manipulators," *Robotica*, vol. 33, no. 1, pp. 1325–1350, 2014.
- [35] Y. Zhang, X. Yan, D. Chen, D. Guo, and W. Li, "QP-based refined manipulability-maximizing scheme for coordinated motion planning and control of physically constrained wheeled mobile redundant manipulators," *Nonlinear Dynamics*, vol. 85, no. 1, pp. 245–261, 2016.
- [36] Y. Shen, P. Miao, Y. Huang, and Y. Shen, "Finite-time stability and its application for solving time-varying sylvester equation by recurrent neural network," *Neural Processing Letters*, vol. 42, no. 3, pp. 763–784, 2015.
- [37] P. Miao, Y. Shen, and X. Xia, "Finite time dual neural networks with a tunable activation function for solving quadratic programming problems and its application," *Neurocomputing*, vol. 143, pp. 80–89, 2014.
- [38] L. Xiao, B. Liao, S. Li, and K. Chen, "Nonlinear recurrent neural networks for finite-time solution of general time-varying linear matrix equations," *Neural Networks*, vol. 98, pp. 102–113, 2018.
- [39] S. Li, S. Chen, and B. Liu, "Accelerating a recurrent neural network to finite-time convergence for solving time-varying sylvester equation by using a sign-Bi-power activation function," *Neural Processing Letters*, vol. 37, no. 2, pp. 189–205, 2013.
- [40] L. Xiao, Z. Zhang, and S. Li, "Solving time-varying system of nonlinear equations by finite-time recurrent neural networks with application to motion tracking of robot manipulators," *IEEE Transactions on Systems, Man, and Cybernetics: Systems*, vol. 22, no. 8, pp. 1–11, 2018.
- [41] Y. Kong, Y. Jiang, and J. Lou, "Terminal computing for Sylvester equations solving with application to intelligent control of redundant manipulators," *Neurocomputing*, vol. 335, pp. 119–130, 2019.
- [42] L. Xiao and Y. Zhang, "From different zhang functions to various ZNN models accelerated to finite-time convergence for time-varying linear matrix equation," *Neural Processing Letters*, vol. 39, no. 3, pp. 309–326, 2014.
- [43] G. Campion, G. Bastin, and B. Dandrea-Novet, "Structural properties and classification of kinematic and dynamic models of wheeled mobile robots," *IEEE Transactions on Robotics and Automation*, vol. 12, no. 1, pp. 47–62, 1996.
- [44] Y. Zhang and Z. Zhang, *Repetitive Motion Planning and Control of Redundant Robot Manipulators*, Springer-verlag, London, UK, 2013.



Hindawi

Submit your manuscripts at
www.hindawi.com

